AN ASYMMETRICAL DUAL BAND BANDPASS FILTER

J.A.G. Malherbe

Department of Electrical, Electronic and Computer engineering, University of Pretoria, Pretoria 2000, South Africa. jagm@up.ac.za.

ABSTRACT: *A dual band bandpass filter consisting of a cascade of unit elements and shunt connected stepped open and stepped short circuited stubs, is described. The dual passbands can have unequal, asymmetrical width; the stop-bandwidth between the desired bands and the harmonic upper bands is substantially increased. A prototype filter that finds application in communication systems is developed .*

Key words: *Dual band bandpass, microwave filter, stepped stub resonators.*

1. Introduction

Dual band bandpass (DBBP) filters find wide application in telecommunications systems such as WiFi, where more than one band of frequencies is of interest. Conventional approaches to the realization of DBBP filters make use of a variety of structures, such as comblines [1], signal interference [2], C-sections [3], spurlines [4], and separate signal paths [5]. An extensive class of structures make use of coupled stepped impedance resonators [6] – [8] or coupled lines [9], multimode resonators [10] – [12] or various stepped stubs or stepped impedance resonators [13] – [17].

In cases where commensurate length circuit elements are used, the passbands are often of equal width, and the responses are repeated harmonically and symmetrically. In this paper, a dual band bandpass filter is described that realizes dual passbands that can differ in relative bandwidth over a wide range, as much as 12:1, while the stopband-width between the upper passband and harmonic passbands is increased.

The filter consists of a cascade of three shunt connected elemental sections separated by sections of cascade transmission line (unit elements), each of length $\lambda_0/2$. The elemental sections each consist of a stepped open circuited stub of total length $\lambda_0/2$, and a short circuited stepped stub of total length $\lambda_0/2$; both stepped stubs are shunt connected to the nodes formed by the unit elements as circuit elements, as shown in Fig. 1(a). The stepped

stubs are cascades of λ/4 lines of different impedance, and this causes the axis of symmetry that would conventionally be formed at $0.5f_0$, to be shifted, resulting in an unsymmetrical response. The response mapped from 0 to f_0 is then mirrored between f_0 and $2f_0$.

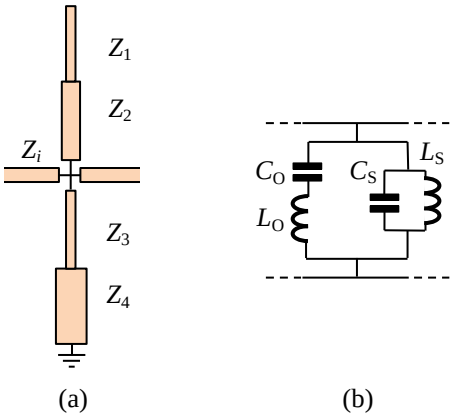

Fig. 1. The elemental OCSS connection. (a) Physical structure. (b) Equivalent circuit.

The stepped open circuited line will force transmission zeros between 0 and f_0, and again between f_0 and $2f_0$, the exact location of the transmission zeros being determined by the relative impedances of the stepped stubs. The stepped short circuited stubs will form transmission zeros at 0 and f_0; passbands are formed to either side of the transmission zeros, and their positions and widths are determined by the relative impedances of the sets of stepped stubs. The passbands properties are determined by the stepped stub impedances, and can be varied over a wide range.

While the physical structure is easily analysed, no procedure exists for the synthesis of the filter from a specification of the desired passband widths, separation, or harmonics. Instead, a heuristic approach to developing a prototype will be followed.

2. Properties of the elemental section

Fig. 1(a) shows a schematic representation of an open circuit stepped stub (OCSS), consisting of unit elements, Z_1 and Z_2, each of length $\lambda_0/4$, shunt connected to a node between two cascade unit elements; a shorted stepped stub (SCSS) with sections Z_3 and Z_4 is connected at the same point. Under Richards' transform [18], the OCSS will cause two transmission zeros on either side of f_0, determined by [19]

$$\begin{aligned} f_{00} &= f_0 \frac{2}{\pi} \tan^{-1} \pm \sqrt{\frac{Z_1}{Z_2}} \\ &= 0.5 f_0 \pm \Delta f \quad \text{and } 1.5 f_0 \mp \Delta f \,, \end{aligned} \tag{1}$$

while the equivalent circuit elements of Fig. 1(b) are given by

$$L_O = \frac{Z_2^2}{Z_1+Z_2},\ C_O = \frac{Z_1+Z_2}{Z_1 Z_2}. \tag{2}$$

The SCSS exhibits a reflection zero at [20]

$$\begin{aligned} f_{00} &= f_0 \frac{2}{\pi} \tan^{-1} \pm \sqrt{\frac{Z_4}{Z_3}} \\ &= 0.5 f_0 \pm \Delta f \quad \text{and } 1.5 f_0 \mp \Delta f\ , \end{aligned} \tag{3}$$

while the equivalent circuit elements are given by

$$C_S = \frac{Y_3^2}{Y_3+Y_4},\ L_S = \frac{Y_3+Y_4}{Y_3 Y_4},\ Y_3 = 1/Z_3,\ Y_4 = 1/Z_4. \tag{4}$$

Transmission zeros are formed at 0, f_0, and $2f_0$.

The equivalent circuit of the shunt connected elemental circuit is shown in Fig. 1(b); Fig. 2 shows an illustrative response with the values of the stepped stubs chosen as $Z_1 = Z_3 = 30\Phi$, and $Z_2 = Z_4 = 70\Phi$, and the cascade unit elements $Z_i = 50\Omega$. For this case the inband transmission zero occurs at $0.3690 f_0$, denoted by the arrow in Fig. 2. The response has an axis of symmetry at $f_0 \propto 4/\lambda_0$; note that the two passbands are unequal, and not symmetrically spaced, while a mirror image is formed about f_0 in the band f_0 to $2f_0$. The choice of (Z_1 - Z_3) and (Z_2 - Z_4) in this example is to a certain extent arbitrary; the major consideration is that Z_1 and Z_2 are different, and that $Z_1 < Z_2$, so as to ensure that the transmission zero falls below $0.5 f_0$. Considerations for the values of Z_i will be discussed later.

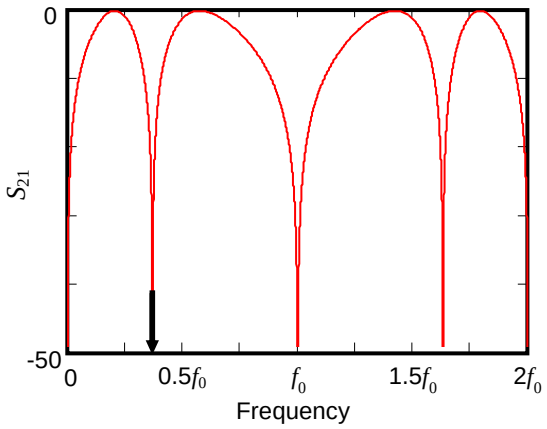

Fig. 2. Elemental section transmission response.

3. Compound Structure

The passband response of the elemental section is dramatically improved by cascading three elemental sections, each separated by a unit element of $\lambda_0/2$, as shown in Fig. 3.

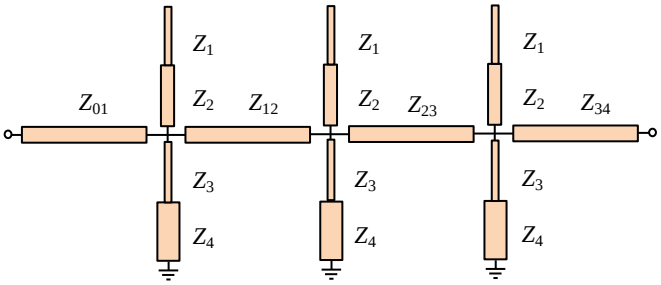

Fig. 3. Physical layout of compound structure.

With the cascade unit elements set to $Z_{01} = Z_{02} = Z_{03} = Z_{04} = 50\Omega$, and the stepped stub impedances $Z_1 = Z_3 = 30\Omega$, $Z_2 = Z_4 = 70\Omega$, as before, the response of Fig. 4(a) is obtained. With adjustment of the unit elements to $Z_{01} = Z_{34} = 90\ \Omega$, $Z_{12} = Z_{23} = 160\ \Omega$, both the passband match and the cutoff rate are dramatically improved, as shown in Fig. 4(b).

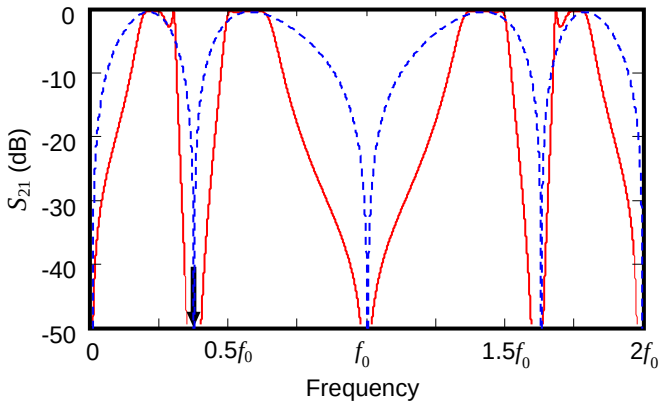

(a)

Fig. 4. Transmission response of compound structure (elemental response shown dashed).
(a) With 50 Ω unit elements; (b) With unit elements adjusted for passband match.

The length of the unit elements is chosen as $\lambda_0/2$ to ensure the correct phase relationship between the cascade of elemental sections, so that the contribution of each section adds constructively. At the same time, cascading the elemental sections cause a substantial mismatch, both internally in the filter, as well as between the filter and the 50 Ω environment. The major contribution of the unit elements in terms of insertion loss, occurs in the vicinity of $0.5f_0$, and its effect on the passband responses can be clearly seen.

4. Element Properties and Development of a Prototype

An exact design procedure for this class of DBBP does not exist. However, evaluation of a large number of prototypes has evolved into a procedure for obtaining a satisfactory filter performance. In the choice of element values, if $Z_1 = Z_2 = Z_3 = Z_4 = Z_{STUB}$, the passbands are approximately equal, and are centered about $f_0/2$ and $1.5f_0$; the response below f_0 is always mirrored above f_0. High values of Z_{STUB} increase the passband widths and low values of Z_i cause narrow bandwidths.

The ratio, Z_1/Z_2 dtermines the position of the transmission zero between the two passbands; to increase the stop-bandwidth between the upper passband and its image, $Z_1 < Z_2$. The position of the zero between the passbands is fixed with fixed Z_1/Z_2; decreasing Z_3 shifts the upper passband, with little effect on the lower passband. A decrease in Z_4 causes the two passbands to shift upwards in frequency; the lower passband is forced closer to the transmission zero, becomes narrower, while the upper passband shifts higher in frequency, and increases in bandwidth.

The internal impedance of filter is substantiall mismatched. Over a wide range of filters it has been found that good starting values are $Z_{12} = Z_{23} = 150\ \Omega$, $Z_{01} = Z_{34} = 80\ \Omega$.

In developing a filter, all stub impedances are initially set equal to 50 Ω, and the unit elements set to $Z_{12} = Z_{23} = 150\ \Omega$, $Z_{01} = Z_{34} = 80\ \Omega$. Now the stub impedances are adjusted: the value of Z_1 is reduced and the value of Z_2 increased to obtain the approximate positions of the passbands. Then Z_3 and Z_4 are adjusted to improve the response towards the desired value. Finally, Adjust the unit element impedances are adjusted to obtain acceptable passband reflection coefficients.

5. Flexibility of Realization

Three examples are included to illustrate the flexibility of the design; examples were chosen to illustrate the wide range of relative bandwidths that are achieved. The element values are given in Table I, as well as the relative bandwidths of the passbands. Fig. 5(a) to 5(c) show the responses for the first passbands, from 0 to f_0. A mirror image is mapped from f_0 to $2f_0$. In the illustrated examples, the ratio of lower passband bandwidth (B_L) to upper passband bandwidth (B_H) varies between $B_L/B_H = 0.18$ and 5.1; ratios between 0.1 and 10 can be readily obtained.

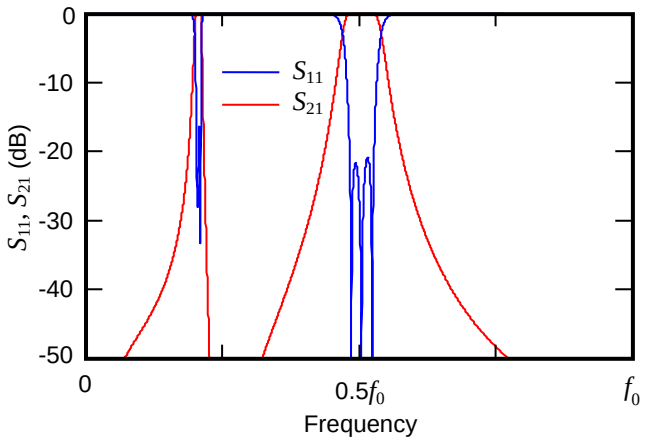

(a)

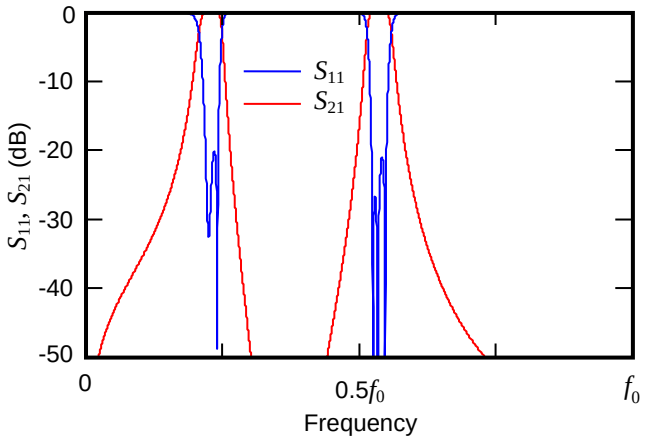

(b)

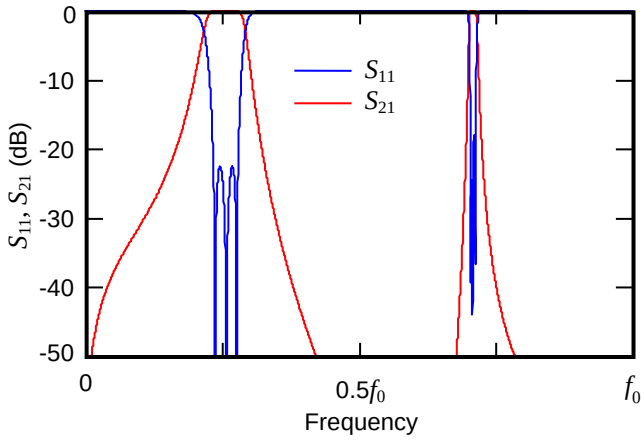

(c)

Fig. 5. Transmission and Reflection Response of illustrative designs. (a) Narrow lower passband, wide upper passband, wide upper stopband. (b) Lower and upper passbands approximately equal, slight reduction in upper stopband. (c) Transmission zero shifted above $0.5f_0$ causes narrow upper passband, reduction in upper stopband.

Table I

Element values (Ω)

Figure	5(a)	5(b)	5(c)
Z_1	20	25	90
Z_2	120	60	40
Z_3	20	20	20
Z_4	30	55	80
$Z_{12} = Z_{23}$	85	83	88
$Z_{01} = Z_{34}$	170	166	168
B_L/f_0 %	1.3	4.3	7.6
B_H/f_0 %	7.1	4.4	1.5
B_L/B_H	0.18	1	5.1

6. Prototype Filter

Following the procedure described above, a prototype was developed for which the theoretical frequency response over a period of $2f_0$ is shown in Fig. 6(a), while the detail of the passbands is shown in Fig. 6(b). Table II shows the element values for the stepped Open circuit (OC) and Short Circuited (SC) stubs, and unit elements.

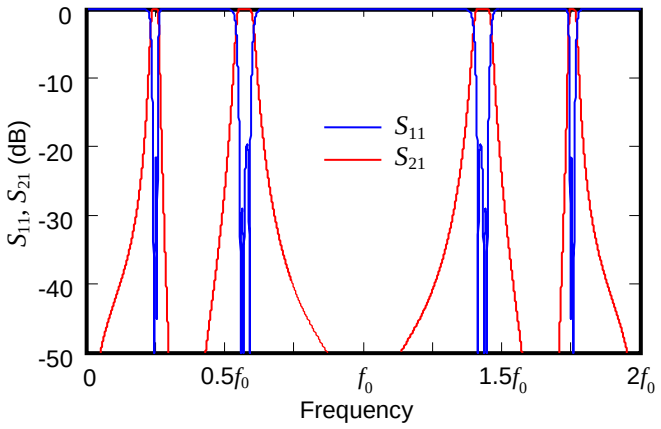

(a)

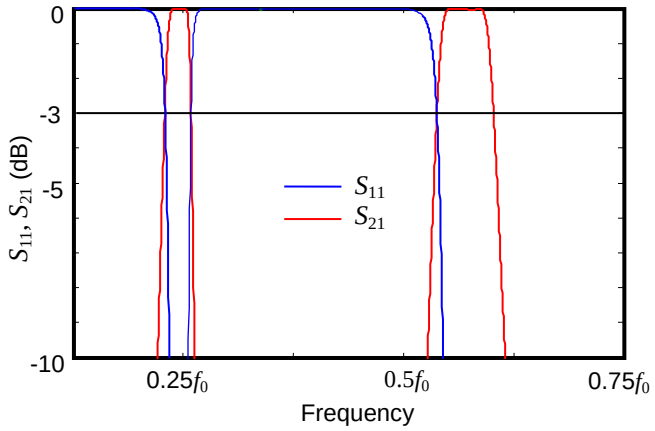

(b)

Fig. 6. Transmission and reflection response of prototype filter. (a) Over a bandwidth of $2f_0$. (b) Expanded view of the passbands.

Table II
Element values for Prototype Filter (Ω)

	Stepped Stub Impedances	Unit Element Impedances
OC	$Z_1 = 24$	$Z_{01} = 83$
	$Z_2 = 70$	$Z_{12} = 165$
SC	$Z_3 = 24$	$Z_{23} = 165$
	$Z_4 = 35$	$Z_{34} = 83$

The filter was constructed as an etched microstrip circuit on RT Duroid 5880, with ε_r = 2.2, and dielectric thickness h = 1.575 mm. Fig. 7 shows a photograph of the constructed filter. As the shorted stubs are all of the same length, they were extended to the edge of the printed board, and the short circuits realized by wrapping copper foil of appropriate width over the ends of the lines and soldering to the ground planes and stubs. The differnce in widths between the various stubs and unit elements are substantial, and were compensated to some extent as shown in Fig. 7; this also applied to end effect compensation.

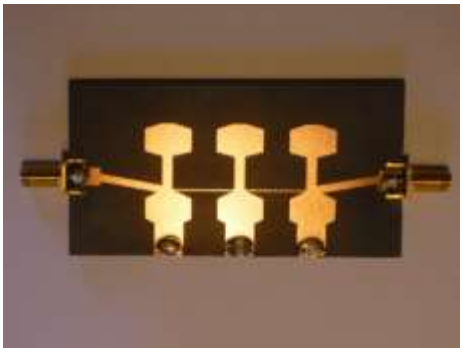

Fig. 7. Manufactured dual band bandpass filter.

The measured reflection coefficient response S_{11} of the filter is compared to the fullwave analysis and the tehoretical response up to the first harmonic response in Fig. 8; the measured transmission and reflection response in the passbands are compared to the theoretical calculations in Fig. 9.

Table III shows a comparison of the measured and theoretical parameters of the filter. The agreement between theoretical and measured parameters is good in the region of the two passbands, and up to the center frequency. Above that, the response diverges from the design

values, due to the substantial discontinuities at the junctions between unit elements and stubs, as well as the fact that no tuning has been performed on this filter.

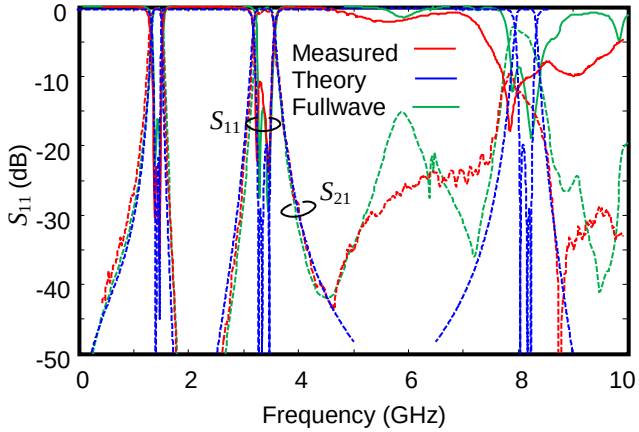

Fig. 8. Comparison of the measured return loss response with the fullwave-analysis and the theoretical values.

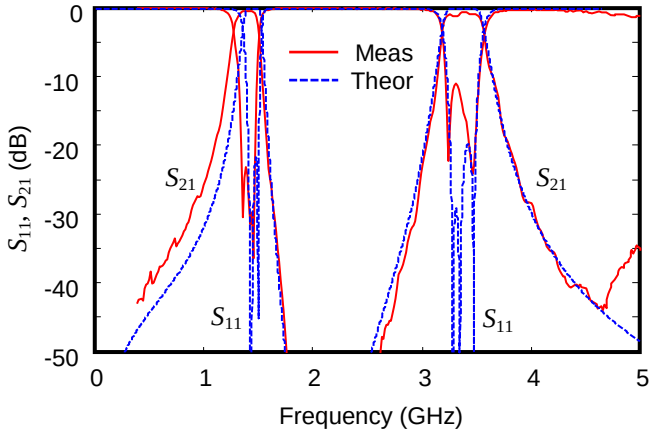

Fig. 9. Comparison of the return loss and transmission Coefficient for the measured and theoretical filter.

Table III
Filter Properties

Variable	Frequency (GHz)	
	Calculated	Measured
f_0	5.926	5.926
B_L	0.177	0.232
f_L	1.445	1.412
B_U	0.382	0.367
f_U	3.378	3.378
B_S	4.714	3.770

In Table III,

f_0 = Centre Frequency
B_L = Lower passband bandwidth
f_L = Lower passband centre frequency
B_U = Upper passband bandwidth
f_U = Upper passband centtre frequency
B_S = Stopband between upper passband and image.

7. Conclusion

In this paper a dual passband filter that employs open and short circuited stepped stubs has been described. A major advantage is that it is possible to realize passbands of different bandwidth, as well as to separate the wanted passbands from the harmonic passbands. This structure is inherently capable of realizing a wide variety of different sets of bandwidths and is of simple construction. Good agreement is found between calculated and measured values.

References

[1] M. Sánchez-Renedo, and R. Gómez-García, "Microwave Combline-Type Dual-Passband Filter," *37th European Microwave Conf 2007*, pp. 321-324.

[2] R. Gómez-García, M. Sánchez-Renedo, B. Jarry, J. Lintignat, and B. Barelaud, "A Class of Microwave Transversal Signal-Interference Dual-Passband Planar Filters," *IEEE Microw Wireless Compon Lett* 19 (2009), 158-160.

[3] Y-C. Chiou, C-Y. Wu, and J-T. Kuo, "New Miniaturized Dual-Mode Dual-Band Ring Resonator Bandpass Filter with Microwave C-Sections," *IEEE Microw Wireless Compon Lett* 20 (2010), 67- 69.

[4] H.W. Liu, Z.C. Zhang, S. Wang, L. Zhu, X.H. Guan, J.S. Lim, and D. Ahn, "Compact Dual-Band bandpass filter using defected microstrip structure for GPS and WLAN applications," *Electron Lett* 46 (2010), 1444-1445.

[5] J-M. Yan, L-Z. Cao, J. Xu, and R-S. Chen, "Design of a Fourth-Order Dual-Band Bandpass Filter With Independently Controlled External and Inter-Resonator Coupling," *IEEE Microw Wireless Compon Lett* 25 (2014), 642-644.

[6] R. Zhang, and L. Zhu, "Design of a compact Dual-Band Bandpass Filter Using Coupled Stepped-Impedance Resonators," *IEEE Microw Wireless Compon Lett* 24 (2014), 155-157.

[7] R. Zhang, and L. Zhu, "Synthesis of Dual-Wideband Bandpass Filters with Source-Load Coupling Network," *IEEE Trans Microwave Theory Tech* 62 (2014), 441-449.

[8] R. Zhang, S. Luo, and L. Zhu, "Asymmetrical-Response Dual-Band Bandpass Filters on λ/8 Transmission Lines With Modified Richard's Transformation," *IEEE Microw Wireless Compon Lett* 24 (2014), 680-682.

[9] Y-H. Cho, and S-W. Yun, "Design of Balanced Dual-Band Bandpass Filters Using Asymmetrical Coupled Lines," *IEEE Trans Microwave Theory Tech* 61 (2013), 2814 - 2820.

[10] R. Zhang, and L. Zhu, "Synthesis and Design of Wideband Dual-Band Bandpass Filters With Controllable In-Band Ripple Factor and Dual-Band Isolation," *IEEE Trans. Microwave Theory Tech* 61 (2013), 1820 - 1828.

[11] L. Gao, and X.Y. Zhang, "High-Selectivity Dual-Band Bandpass Filter Using a Quad-Mode Resonator With Source-Load Coupling," *IEEE Microw Wireless Compon Lett* 12 (2013), 474 – 476.

[12] S-J. Sun, T. Su, K. Deng, B. Wu, and C-H. Liang, "Compact Microstrip Dual-Band Bandpass Filter Using a Novel Stub-Loaded Quad-Mode Resonator," *IEEE Microw Wireless Compon Lett* 23 (2013), 465-467.

[13] S. Yang, L. Lin, J. Chen, K. Deng, and C-H. Liang, "Design of compact dual-band bandpass filter using dual-mode stepped-impedance stub resonators," *Electron Lett* 50 (2014), 611-613.

[14] S. Zhang, and L. Zhu, "Synthesis Design of Dual-Band Bandpass Filters With λ/4 Stepped-Impedance Resonators," *IEEE Trans Microwave Theory Tech* 61 (2013), 1812 - 1819.

[15] S. Zhang, and L. Zhu, "Fully canonical dual-band bandpass filter with λ/4 stepped impedance resonators," *Electron Lett* 50 (2014), 192-194.

[16] J. Luo, C. Liao, H. Zhou, and X. Xiong, "A Novel Miniature Dual-Band Bandpass Filter Based on the First and second resonances for 2.4-5.2 GHz WLAN Application," *Microw Opt Tech Lett* 57 (2015), 1143-1146.

[17] H. Cui, Y. Sun, S. Wang, and Y. Lu, "Dual-Band Differential Bandpass Filter Using Stepped Impedance Resonators," *Int Jnl RF Microwave Computer-Aided Eng* 25 (2015), 468 - 473.

[18] P.I. Richards, "Resistor-Transmission-Line Circuits," *Proc IRE* 36 (1948), 217 – 220.

[19] J.A.G. Malherbe, P.D. Luus, and J.C. Uys, "Transmission Line Filters With Harmonic Parallel Foster Sections," *Microw Opt Tech Lett* 55 (2013), 1724 – 1728.

[20] J.A.G. Malherbe, "Dual Band Bandpass Filter with Shunt Shorted Stubs," *15th Int Symp Microwave Opt Tec, ISMOT 2015*, Dresden, Germany, 2015, pp.156-159.